A laser thermal cycling rig as a new method to characterize the evolution of coating adhesion under thermal cycle

Poirier, D.; Irissou, E.; Legoux, J. G.

Publisher's version / Version de l'éditeur:

Thermal Spray 2012 : Proceedings from the International Spray Conference, pp. 137-142, 2012-05-21

A Laser Thermal Cycling Rig as a New Method to Characterize the Evolution of Coating Adhesion under Thermal Cycle

D. Poirier*, E. Irissou, J.G. Legoux
National Research Council of Canada (NRC), Boucherville, Quebec, Canada
**E-mail: Dominique.Poirier@cnrc-nrc.gc.ca*

Abstract

Thermal sprayed coatings are often used for high temperature applications and, per se, are subjected to transient temperature gradients during operation. The recurrent temperature changes generate stresses that damage the coating with time, and can even lead to its delamination. The most common methods to evaluate coating behavior under thermal cycling are furnace testing or burner rigs. Both approaches can not match the conditions reached in service for several applications, in term of the achievable heating rates for instance. As a consequence, a versatile and robust method to evaluate coating resistance to spalling under thermal cycles is still to be found. This paper presents the development of a thermal cycling rig where the heat input is provided by a laser. This rig allows easy testing of several samples jointly for heating rates as high as 55°C/s and for thousands of thermal cycles. Preliminary trials have allowed the development of different spalling criteria. Finally, it was found that SS430-based materials arc-sprayed on Al substrates exhibit higher delamination resistance (life) under rapid heating/cooling cycles than SS304 coatings on the same substrate. For such high heating rates, the thermal stresses generated in the coating would be more critical than the thermal mismatch at the interface coating/substrate.

Introduction

Thermal sprayed coatings are often used for high temperature applications and, per se, are subjected to transient temperature gradients during operation. Coating resistance to thermal spalling is particularly critical for applications where severe thermal cycles are present, such as aircraft and land-based turbines (Ref 1, 2), diesel engines (Ref 2, 3) and steam valves used in the chemical industry and power plants (Ref 4). In those cases, a good understanding of coating behavior under thermal cycling is critical to avoid coating spalling and catastrophic failure. In order to replicate those thermal cycles in laboratory conditions, heating in a furnace or with the help of a burner rig is typically performed. While furnace tests are low cost and can be tightly and easily controlled, this method is limited by the low heating rates achievable, in the order of a couple of degrees Celsius per second (Ref 5). In addition, they are imposing minimal thermal gradient across the coating. A burner rig can achieve pronounced temperature gradients and somewhat faster heating rates but it still can not match some of the highest heating rates reached in service. The thermal cycles are performed in a combustion atmosphere, which is non-representative of several applications. Furthermore, the burner rig does not allow accurate measurement of the temperature profiles (Ref 1). As a consequence, a versatile and robust method to evaluate coating resistance to spalling under thermal cycles is still to be developed.

For a couple of decades, laser heating has been employed in experimental set up for material fundamental research such as creep mechanism analysis (Ref 6) or single thermal shock studies (Ref 7). Lately, heating coated samples through a moving laser shot has been investigated as a possible burner rig alternative (Ref 8). However, the laser motion on the sample surface has lead to uneven temperature distribution. A subsequent study using a laser with a broad focal point looked promising (Ref 9), but only a few thermal cycles were performed per coating, probably due to the limiting set up. This paper presents the development of a new thermal cycling rig where the heat input is provided by a laser. After the presentation of the rig design itself, preliminary results are shown regarding the temperature cycles achievable with the rig. Potential delamination identification methods are assessed and compared. Finally, the variations in the adhesion of arc-sprayed metallic coatings subjected to thermal cycling are reported.

Thermal Cycling Rig Design

Overall Thermal Cycling Rig Principles

In this thermal cycling rig, coated samples are successively heated by a YAG laser and cooled down by air flow through the motion of a sample holder. In the current design, three samples are attached to the sample holder: once the first sample is heated, it is moved to the cooling down region while

the next sample is being heated (Fig. 1). All process devices are thus stationary and enclosed in a chamber equipped with interlock doors and tinted windows for laser safe handling. The process monitoring and control is performed with Labview software (National Instrument, Austin, USA) from a computer outside the booth. The entire system is illustrated in Fig. 2 and a picture of the main components is shown in Fig. 3.

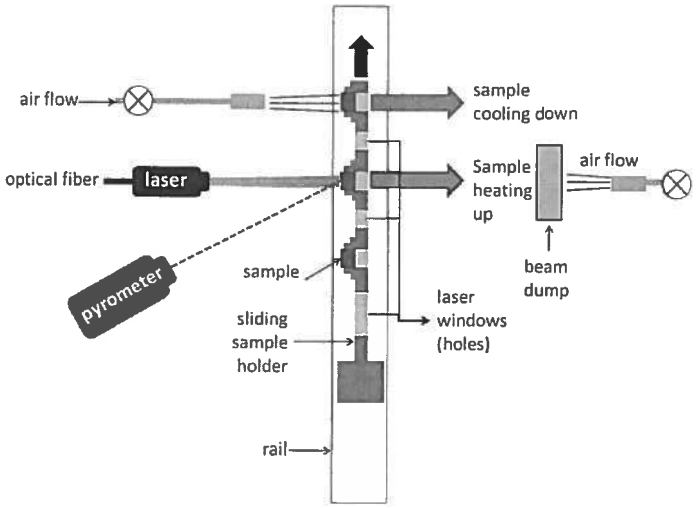

Figure 1: Layout of the sample setting and the surrounding apparatus

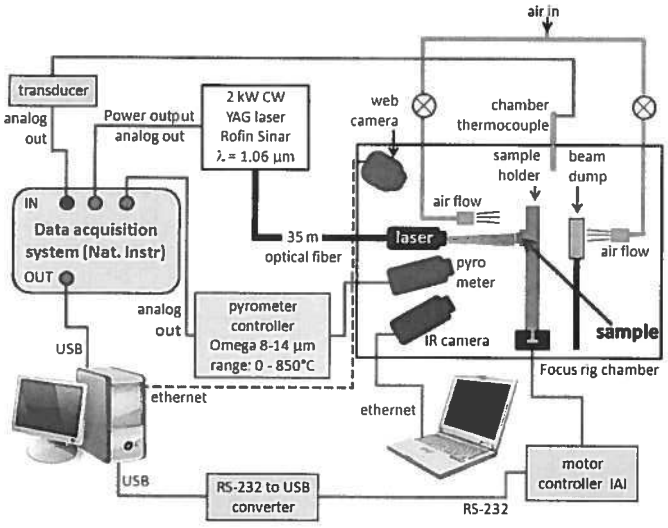

Figure 2: Block diagram of the entire thermal cycling rig

Heating and Cooling Zones

A specimen is first heated from the coated surface with a 2 kW CW YAG laser (Rofin Sinar, Hamburg, Germany) whose power can be adjusted to obtain the desired heating rate. As this laser is continuously on during the tests, a beam dump cooled down by an air flow has been added to collect the heat input in between heating steps.

The specimen is then quickly moved to the cooling zone where compressed air is directed to the coated surface. Natural cooling is pursued in the standby zone and as the sample holder location is reinitialized to start a new cycle. A cylindrical robot (IAI America, Torrance, USA) is used to move the sample holder.

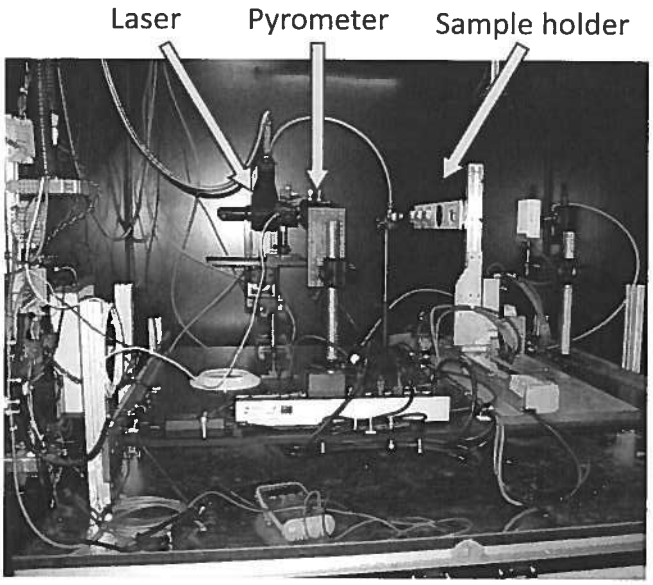

Figure 3: Picture of the actual rig

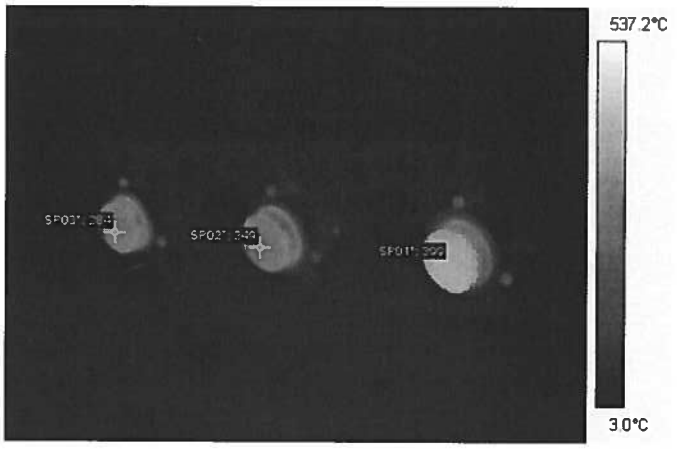

Figure 4: Infrared camera picture of the samples after some heating. On the picture, temperatures are indicated on three spots: Spot 1 is located on the sample being heated, spot 2 on the sample being cool down and spot3 on the standby sample.

Process Monitoring

A pyrometer operating at a wavelength range of 8-14 µm for a calibrated temperature range of 0-850°C (Omega, Stamford, USA) is recording the temperature of the sample being heated.

The collected data are transferred to the main computer through the data acquisition system (National Instrument, Austin, USA). The three samples are also filmed by a A320 infrared camera (Flir, Boston, USA) as well as a webcam (Toshiba, Tokyo, Japan) on which a neutral density filter 1 µm has been added. As shown in Fig. 4, the temperatures of three spots corresponding to three critical steps of the process are recorded from the infrared camera data. As the heating is performed in a close chamber, a thermocouple was added to monitor possible increase in ambient temperature during experiment.

Preliminary Trials

Arc-sprayed samples were produced for preliminary thermal cycling trials. Praxair 80T and 61T wires were arc sprayed on degreased and grit blasted A356 cylinders 25.4mm dia X 16 mm height using the SmartArc(SA) or the Miller (M) system following the conditions shown in Table 1. 80T wire composition is equivalent to stainless steel(SS) 304, with a coefficient of thermal expansion(α) of $17.3X10^{-6}$/°C, while 61T wire composition is equivalent to SS430, α of $10.3X10^{-6}$/°C (Ref 10). The thermal expansion coefficient of the aluminum substrates is $21.5X10^{-6}$/°C (Ref 11). Coating thicknesses varied between 400 and 500 µm. As-sprayed adhesion values were evaluated according to modified ASTM-C633 standard: the coated Al samples were glued on each side to standard mild steel pull test studs for tensile testing. The results are shown in Fig. 5. Coating emissivity was measured to be 0.84.

Table 1: Spraying parameters

Gun	SA	M
Current	100 A	100 A
Voltage	28 V	28 V
Spraying Distance	15 cm	10 cm
Gas Pressure	60 psi	60 psi
Traverse speed	75 cm/s	75 cm/s

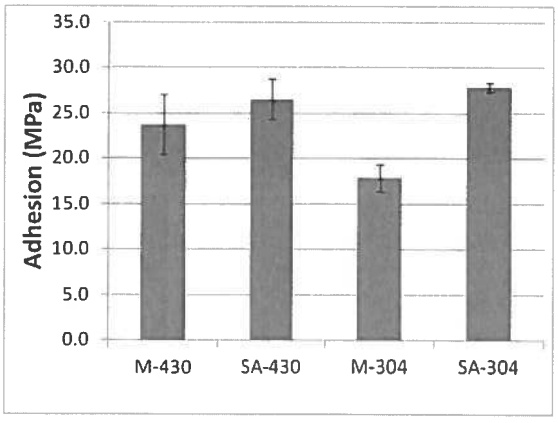

Figure 5: As-sprayed coating adhesion

For those preliminary trials, a heating rate of at least 40°C/s and a final heating temperature of about 450°C were targeted. It was defined experimentally that a laser power of 1300W and a heating time of 4 s. were offering satisfactory results.

Results and Discussion

Characterization of thermal cycles:

Due to the rig set up for which the samples are moving, the recorded temperature profiles obtained by the infrared camera or the pyrometer correspond to a location, and not a specific sample. Therefore, the temperature profiles of three different spots (shown in Fig 4.), chosen to match the three critical steps of the process, i.e. heating up, cooling down and stand by, must be compared to get a representative idea of the actual thermal cycles withstand by the coated samples. Figure 6 shows the temperature profiles obtained from the infrared camera by the testing of 3 arc-sprayed samples. For the heating up and cooling down stages, each cycle composed of 3 samples are easily delimited. For the standby stage, the temperature variations of only two samples per cycle are visible: this is caused by the sample holder motion as its position was immediately reinitialized after cooling down of the third sample. At steady state, a maximum temperature of 470°C is obtained as seen in spot 1, with a heating rate of about 50-55°C/s. This heating rate is well above the targeted heating rate and could be further increased by increasing the laser power. The minimum sample temperature is about 250°C as seen in spot 3.

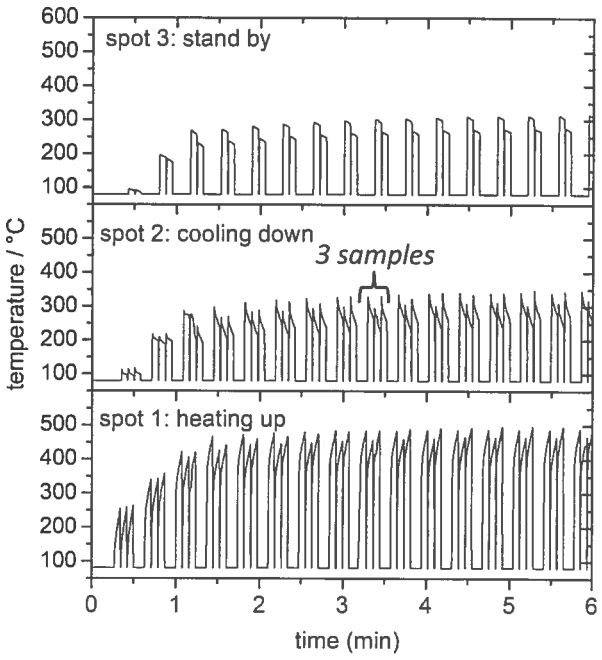

Figure 6: Temperature variation with time recorded on three locations with the infrared camera

The pyrometer recorded temperature profile, shown in Fig.7, is similar to the one obtained with the infrared camera for spot 1, i.e. a maximum temperature of about 500°C. The slight difference could be due to the size of the spot which is bigger in the case of the pyrometer or to the processing time which is longer in the case of the pyrometer.

Also in Fig.7, the chamber temperature was shown to increase to reach about 32°C and then stabilize after further testing, indicating sufficient ventilation of the booth.

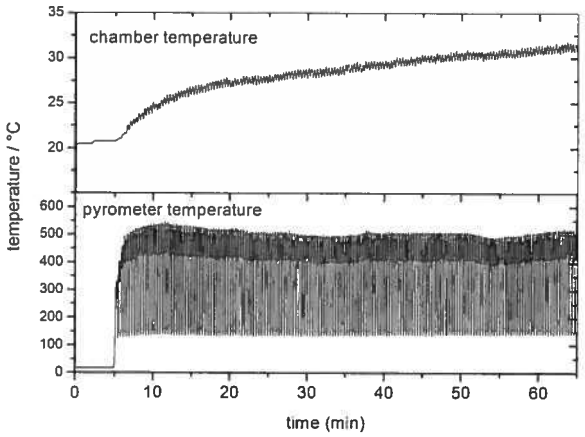

Figure 7: Temperature variation with time recorded by the chamber thermocouple and the pyrometer

Delamination Identification

In order to compare the thermal shock resistance of the different coatings, two routes were foreseen: either subject all coatings to a specific number of cycles and measure their decrease in adhesion with standard pull test procedure or cycle the coatings until failure and compare the number of cycles achieved for each coating. In the later case, delamination identification methods had to be developed. Two efficient ways are presented in the followings.

It was noticed on the infrared camera or the webcam that hot spots could appear on the coating in the heating zone upon cycling (Fig. 8). Those hot spots were associated to the partial delamination of the coating, creating a gap of low thermal conductivity between the coating and the substrate and thus a higher surface temperature. One identification method was then to record to number of thermal cycles needed to reach 25% hot spot on the surface of the coating.

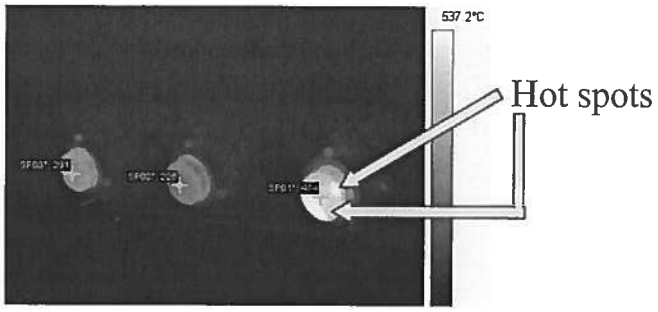

Figure 8: Infrared camera picture showing the presence of hot spots on the sample.

The same phenomena of surface temperature increase could also be measured with the pyrometer. As shown in the temperature profile close up of Fig. 9, the maximum surface temperature of sample 3, and to a lower extent the one of sample 1, is higher than for sample 2, which was not delaminated. Looking to the entire thermal history on Fig. 10, it can be seen that once delamination has started, the surface temperature of the sample keeps increasing until the end of the test. The time when the measured surface temperature starts to increase can easily be point out, i.e. 560 cycles for sample 3 and 570 cycles for sample 2. This represents the time for the onset of coating delamination.

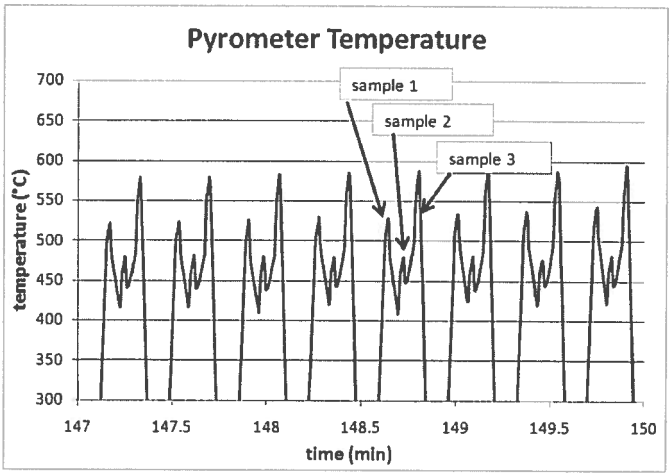

Figure 9: Temperature variation with time recorded by the pyrometer. The presence of hot spots on sample 3 is recorded as an overall increase in temperature of this sample compared to the other samples.

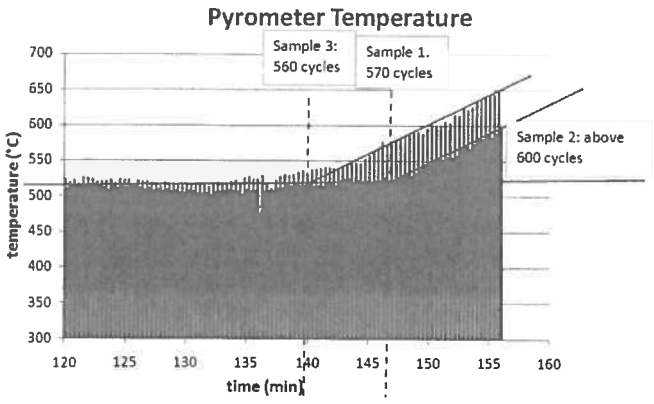

Figure 10: Temperature variation with time recorded by the pyrometer. Number of cycles prior to delamination can be identified.

Adhesion Results

Initial adhesion results were obtained from the arc-sprayed samples. For those preliminary tests, the number of cycles for the first sample to reach 25% hot spot was chosen as the spalling criteria for its ease of use and in order to limit the number of thermal cycles required.

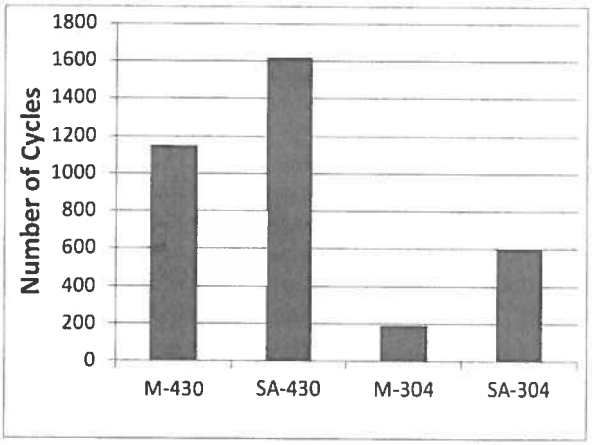

Figure 11: Thermal cycling test results. The number of cycles for the first sample to reach 25% hot spot has been recorded for each coating type.

From Fig.11, it can first be noticed that the coatings produced with the SA display a higher resistance to spalling under thermal cycles. This is probably due to the superior initial adhesion of those coatings (Fig. 5). Also, the coatings produced with SS430 (α of $10.3X10^{-6}/°C$) wire exhibit higher spalling resistance than those with SS304 (α of $17.3X10^{-6}/°C$).

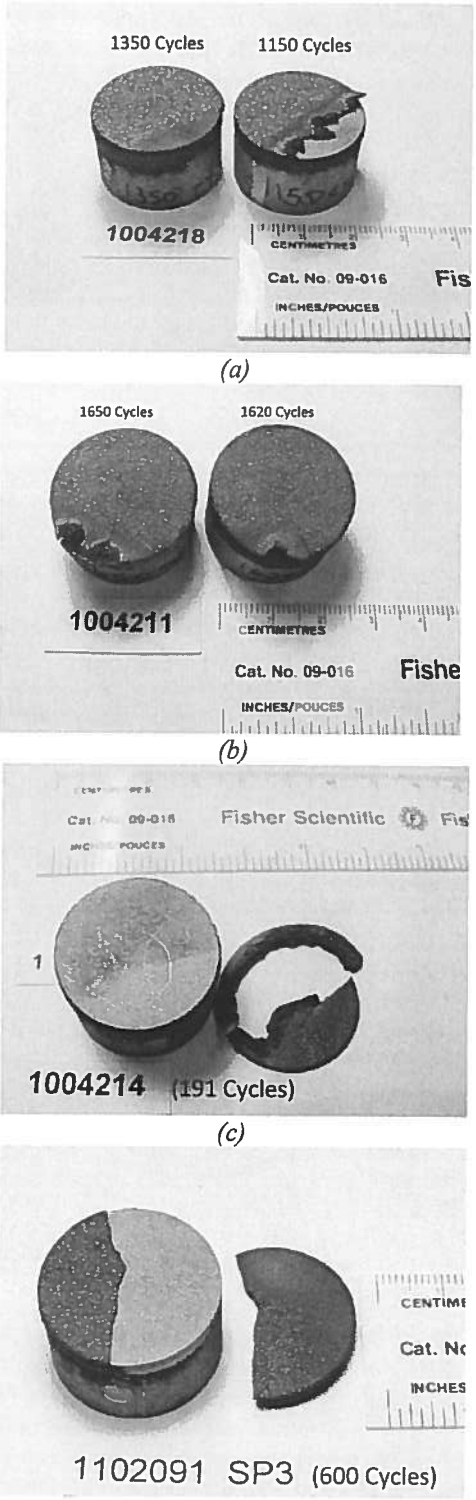

Figure 12: Coated samples after thermal cycling (a) M-430 (b) SA-430 (c) M-304 (d) SA-304

Figure 12 is showing the samples after thermal cycling. The SS304 coatings have been highly damaged and in one case (M-304), the coating totally delaminated after final cooling down. This behavior may be counter intuitive since SS304 has a thermal expansion coefficient closer to the one of the aluminum substrate. It can be envisioned that different thermal stresses could be generated between the coating and the substrate by varying the temperature cycling conditions. Using very short heating time, the high temperature zone can be limited to the coating. Thermal strains are then a function of the coating temperature and expansion coefficient only. However, for longer heating time, the high temperature zone can reach the substrate; in such a case, thermal mismatch would be a function of the difference of thermal expansion coefficients between the coating and the substrate.

It is thus believed that the lower thermal expansion coefficient of the SS430 coatings reduces the thermal stresses within the coating and helps preserving its integrity. On the other hand, SS304 offers a better thermal expansion coefficient match with the A356 substrates. This should minimize the thermal stresses at the coating/substrate interface in the case of more prolonged thermal exposure. More work on this aspect is required in order to verify this point.

Conclusions

In this study, a versatile and robust test rig to evaluate coating resistance to spalling under thermal cycles has been elaborated. Coated samples are successively heated by a YAG laser and cooled down by air flow through the motion of a sample holder for thousands of cycles and with heating rates as high as 55°C/s. Spalling criteria based on visual inspection and infrared camera or pyrometer monitoring have been developed. Preliminary results show that 430-based coatings (low α) produced on Al substrate exhibit higher delamination resistance under rapid heating/cooling cycles than 304-based coating (high α offering better match with the substrate). This finding is valid for short heating times. In those cases, only the thermal expansion coefficient of the coating would need to be considered because the high temperature zone would not reach the interface coating/substrate. Testing involving slower thermal cycling is to be undertaken to validate this hypothesis.

Acknowledgement

The authors would like to thank Bernard Harvey and Mario Lamontagne for their essential help in the design, fabrication and operation of the thermal cycling rig. The authors would also like to thank Frédéric Belval for sample production as well as Marie-Lise Tremblay for her instructive comments.

References

1. R. Miller, Thermal barrier coatings for aircraft engines: history and directions, *J. Therm. Spray Technol.*, 1997, **6**(1), p 35-42
2. S.L. Chawla, R.K. Gupta, Materials selection for corrosion control, ASM International, Novelty, USA, 1993
3. T. Hejwowski and A. Weroński, The effect of thermal barrier coatings on diesel engine performance, Vacuum, 2002, 65(3–4), p 427-432
4. L. Vernhes, D.A. Lee, D. Poirier, J. Sapieha, D. Li, HVOF Coating Case Study for Power Plant Process Control Ball Valve Application, for publishing in the same issue.
5. M. Matsumoto, H. Takayama, D. Yokoe, K. Mukai, H. Matsubara, Y. Kagiya, and Y. Sugita, Thermal cycle behavior of plasma sprayed La2O3, Y2O3 stabilized ZrO2 coatings, *Scripta Mater.*, 2006, **54**(12), p 2035-203
6. W. Pompe, H.A. Bahr, I. Pflugbeil, G. Kirchhoff, P. Langmeier, and H.J. Weiss, Laser induced creep and fracture in ceramics, *Mater. Sci. Eng. A*, 1997, **233**(1–2), p 167-175
7. S. Rangaraj and K. Kokini, Fracture in single-layer zirconia (YSZ)–bond coat alloy (NiCoCrAlY) composite coatings under thermal shock, *Acta Mater.*, 2004, **52**(2), p 455-465
8. D. Nies, R. Pulz, S. Glaubitz, M. Finn, B. Rehmer, and B. Skrotzki, Testing of Thermal Barrier Coatings by Laser Excitation, *Adv. Eng. Mater.*, 2010, **12**(12), p 1224-1229
9. J. Schloesser, M. Bäker, and J. Rösler, Laser cycling and thermal cycling exposure of thermal barrier coatings on copper substrates, *Surf. Coat. Technol.*, 2011, **206**(7), p 1605-1608
10. P. D. Harvey, *Engineering properties of steel*, American Society for Metals, Ohio, USA, 1982
11. W.D. Callister, *Materials Science and Engineering; An Introduction,* John Wiley & Sons, New York, USA, 2000